Overview of NEO-related research by the Planetary Science Team at University of Alicante (Spain)

IAA-PDC-25-05-196

Adriano Campo Bagatin[a,b,g] (acb@ua.es), Toni Santana-Ros[b,c], Laura M. Parro[a], Stephen R. Schwartz[a,d], Po-Yen Liu[a], Nair Trógolo[a,e], Przemysław Bartczak[a,f], Paula Benavidez[a,b], Manuel Perez-Molina[a,b]*

[a] *Instituto Universitario de Fisica Aplicada a las Ciencias y a las Tecnologias, Universidad de Alicante, Spain.*
[b] *Departamento de Fisica, Ingeniería de Sistemas y Teoría de la Señal, Universidad de Alicante, Spain.*
[c] *Institut de Ciències del Cosmos (ICCUB), Universitat de Barcelona (IEEC-UB), Spain.*
[d] *Planetary Science Institute, Tucson, AZ, USA.*
[e] *Universidad Nacional de Córdoba, Argentina.*
[f] *Astronomical Observatory Institute, Faculty of Physics, A. Mickiewicz University, Poznan, Poland.*
[g] *Dipartimento di Fisica e Astronomia "Galileo Galilei", Università degli Studi di Padova, Italy*

DFISTS
Dpto. Física, Ingeniería de Sistemas y Teoría de la Señal
UA UNIVERSITAT D'ALACANT UNIVERSIDAD DE ALICANTE

Asteroid internal structure determination

In the frame of the Hera (ESA) and RAMSES (ESA) space missions, **we combine** our models of asteroid internal structure with realistic, irregular components (INSIDE) + efficient gravity field calculation (OUTSIDE) **with** information from spacecraft measurements at different mission phases.
We improve the mission target internal structure determination by iterating over modelling and measurements.

Hera mission (ESA)

Phase	Instrument	Data	Information	Missing info	Algorithm	Outcome
1. ECP	AFC + PALT + HyperScout	Volume. Mass. => Shape model. Spectral type.	Volume & mass. Bulk density (Didy & Dimo). Material density. Macro-porosity.	Mass gross distribution. SFD of Components. Internal texture. Detailed G-field.	INSIDE	Multiple models with constant bulk density
2. DCP	X-DSL + ISL	ÞJ2 (0.1-10%). ÞG-field to deg 2-3 (~10%).	Gross mass distribution ~ρ(r). Constraints on SFD.	SFD of Components. Internal texture. Detailed G-field.	INSIDE + OUTSIDE	Models with limited SFD options
3. COP	JuRa	Backscatter coeff. Dielectric constants è permittivity contrast	Int. distr. voids and mass (Res ~10 m) on Dimorphos & partially on Didymos.	Detailed G-field	INSIDE + OUTSIDE	Models with given SFD, degeneracy on components position in Didymos
4. EP	GRASS	g accel. on Dimorphos surface.	G-field on a full period (Res < 0.05 mGal)	-	INSIDE + OUTSIDE	Definitive model for Didymos and Dimorphos.

Analysis of asteroid surface features

A different way of **characterizing the interior of asteroids is based on interpretations of their surface properties**. This fundamentally impacts how different small body reservoirs formed and evolved and how different surface geomorphologies form.

Consequently, **we map, analyse, and compare different surface features** (e.g., boulders, fractures, cracks, lineaments, pits chains, impact craters, etc.) to explore the **geological evolution** of each body continuously, and the **possible correlation of such features with their physical properties.**

For example, **asteroids of tens of kilometers and larger** show characteristic **linear features**, possibly formed by the drainage of regolith in subsurface extensional fractures. In contrast, the identification of linear structures on the surface of **smaller asteroids** (**rubble-pile structures**) has probably not been as straightforward due to their **low internal strength**. Even in this regime, the **composition of each body can make some difference in the observed geological features**, for example, between the S-class asteroids (e.g., Itokawa, Didymos/Dimorphos) and the B- and C-class asteroids (like Bennu or Ryugu).

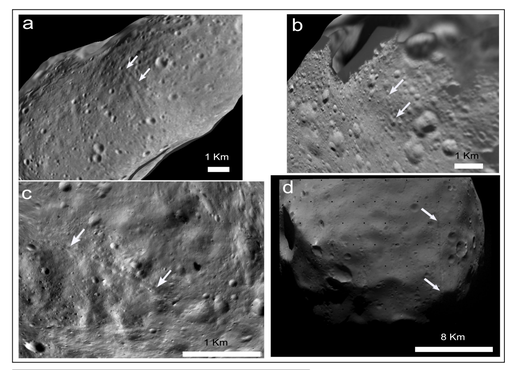

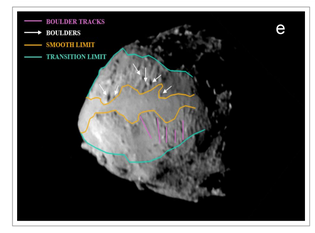

Arrows mark the position of different lineament features in the surfaces of a) Gaspra; b) Ida; c) Eros; and d) Phobos (de Luis and Parro, 2025). In the case of panel e) (Trógolo et al., under review), the Didymos asteroid image marks the geological unit limits and the possible position of individual boulders and their corresponding tracks (Barnouin et al., 2024).

Formation of near-Earth binary asteroids

⇒ **Please, check poster IAA-PDC-25-06-241:**

Liu, P.-Y., et al.
Collisional Spin-Up of Asteroids: Alternative Mechanisms of Binary Asteroid Formation Independent of YORP Effects

Particle dynamics in the Didymos environment

⇒ **Please, check poster IAA-PDC-25-05-188:**

Trogolo, N., et al.
Mass ejection by fast-spinning Didymos: orbiting dust and transference to Dimorphos

Fast gravity computation (OUTSIDE) and surface stability analysis

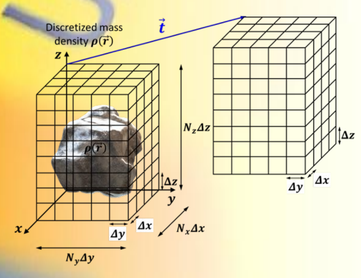

The density of a given arbitrary body is discretized in a grid of $N_x \times N_y \times N_z$ cells with edges Δx, Δy, Δz. The gravity field is computed fastly and accurately at all points of the grid translated by any vector $\vec{t}$ using FFT.

Aggregate made up 447 irregular fragments (189004 spheres)

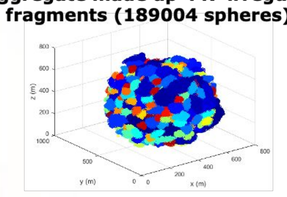

Gravity field modulus at equatorial plane (ms^{-2})

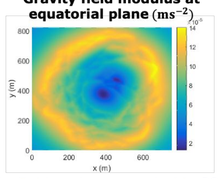

Gravity field vector computed in 29 s (CPU: 16 GB RAM memory)

Different structures can be resolved in terms of *G*

Distance from mass center	Required accuracy
550 – 600 m	~ 1 mGal
1.2 – 1.4 km	~ 0.02 mGal
2.5 – 2.7 km	~ 2 μGal

Super-ellipsoids reproduce shape models and slope angle (surface stability)

$$\left|\frac{x}{a}\right|^n + \left|\frac{y}{b}\right|^n + \left|\frac{z}{c}\right|^n = 1$$

Top-shapes are more stable (smaller slope angles) than ellipsoidal bodies at fast rotation

Slope angle (°) for polyhedral shape models spinning at 97 % spin rate detachment

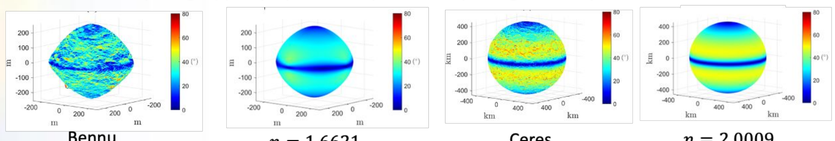

Effects of slow-speed boulder impacts on the Didymos system after DART

Secondary impact cratering is the result of excavated material from a larger impact that then re-collides with the surface, found within the radius of the ejecta blanket of the primary impact.

In the case of DART, this ejecta blanket may cover the entire surface of Dimorphos.

Owing to the relatively small sizes of Dimorphos and Didymos, dynamical simulations show that typical re-impact speeds would be small, comparable to the escape velocity of the the body or system, under 1 m/s.

We are using granular dynamics models to investigate the behavior of these impacts and their tell-tale signatures, which may be recognized by the Hera spacecraft.

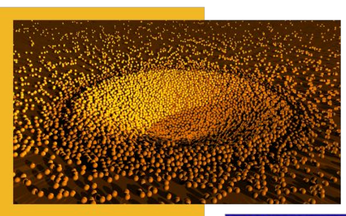

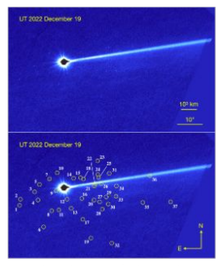

Jewitt et al. (2023)

- Using HST images of the DART impact event, an extensive population of comoving boulders was discovered.
- Largest boulder ~7 m
- 37 boulders measured
- Mean sky-plane velocity dispersion of 30 cm/s +/- 10%
- Collective mass ~5 M kg assuming 2.2 g/cc
- Long-term orbital evolution analyzed by Moreno et al (2024); Langner et al. (2024).

Determining the physical parameters of NEOs

To characterize the physical parameters of Near-Earth Objects (NEOs), we utilize a comprehensive suite of observational data, including **rotational lightcurves, radar measurements, sparse photometry from wide-field surveys, and astrometric data** (e.g. from the Gaia sky survey).

These diverse datasets **provide complementary constraints on the shape, rotation state, and surface properties of NEOs**. We employ the **SAGE** lightcurve inversion technique and the **SHAPE** modeling software to model these observations, enabling robust three-dimensional shape reconstructions and spin-state determinations.

Furthermore, **we apply corrections for the displacement between the photocenter and the center of mass**, which are critical for accurate orbit determination. These corrections, in turn, **enhance our ability to quantify non-gravitational forces such as the Yarkovsky effect and to estimate the bulk density of the objects**. This integrated approach advances our understanding of the dynamical and physical evolution of potentially hazardous asteroids.

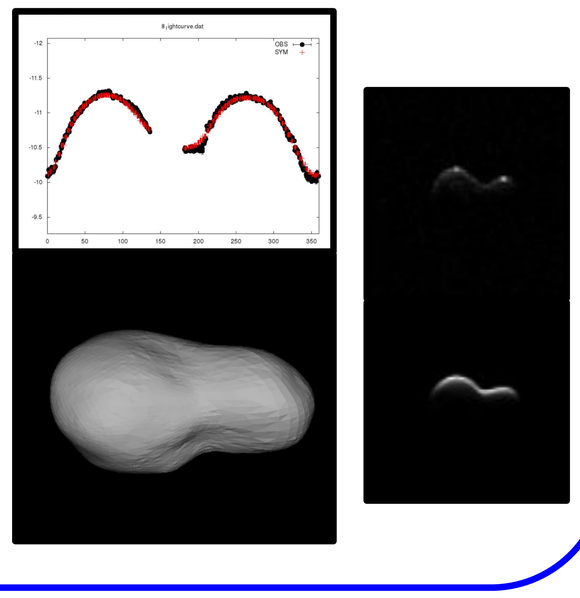

Inner Earth Objects (IEO) survey

To date, we have discovered **35 objects following Interior Earth Orbits** (IEOs)—trajectories entirely contained within Earth's orbit. While these objects do not pose an immediate impact risk, **gravitational perturbations**—especially from close encounters with Mercury and Venus—**can alter their orbits over time, potentially shifting them into Earth-crossing paths**. Early identification and continuous monitoring of IEOs are critical for assessing long-term impact probabilities and enhancing planetary defense strategies.

However, major sky surveys are not optimized to detect these objects: IEOs are **only visible at low solar elongations**, meaning they appear close to the Sun and are best observed during twilight hours. This presents significant observational challenges, such as limited viewing windows, high sky brightness, and special telescope requirements, including the ability to point at low elevations.

To overcome these limitations, **we have launched two coordinated twilight survey programs**. The first uses the Telescope Fabra ROA Montsec (**TFRM**), located in Catalonia, Spain, covering the Northern Hemisphere. The second employs the **Springbok** telescope in Namibia, providing complementary coverage from the Southern Hemisphere. Operating in parallel, these surveys increase the likelihood of detecting IEOs. To optimize our observing strategy, **we have developed dedicated software** (see figure on the right) that selects suitable fields based on a set of constraints—such as solar elongation limits, minimum visibility duration—for a given date and location.

Our goal is to systematically expand the IEO catalog, study their orbital evolution, and physically characterize their members.